

Supporting Information

High Frequency Capillary Wave Enabled Ultra-small Droplets for Inhaled Drug Delivery

Haitao Zhang¹, Zirui Zhao¹, Yangchao Zhou¹, Zaoxian Mei² and Xuexin Duan^{1*}

¹State Key Laboratory of Precision Measuring Technology & Instruments, and College of Precision Instrument and Opto-electronics Engineering, Tianjin University, Tianjin 300072, China

²Tianjin Hospital, Tianjin 300211, CHINA

1. Design and fabrication of high frequency acoustic resonator

The fabricated acoustic resonator and its structure are shown in Fig. S1.

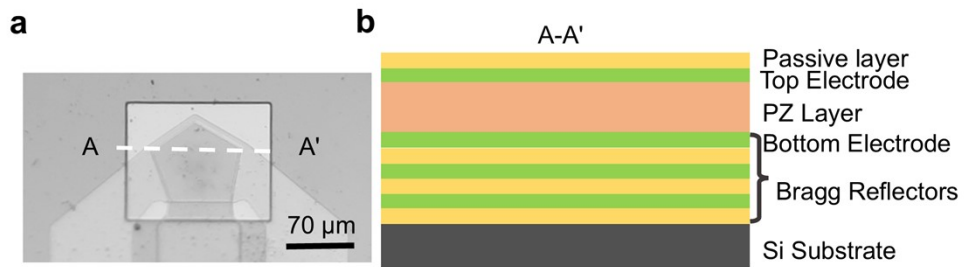


Fig. S1: (a) Enlarged view of the GHz acoustic resonator. (b) Schematic sectional view of section A-A'.

2. Portable nebulizer

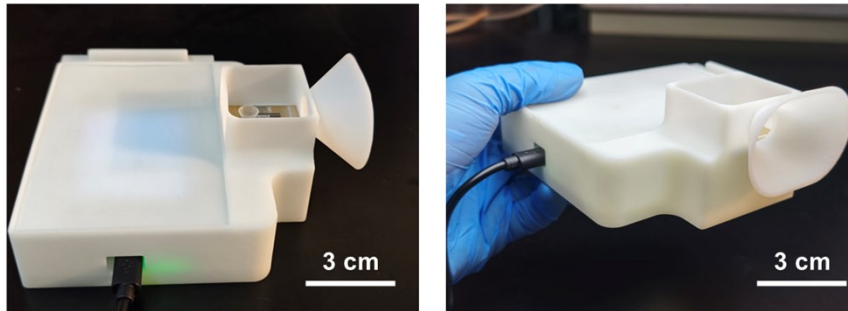


Fig. S2: Image of a small driving circuit fabricated as a power source for the portable nebulizer.

3. Human lung model test

A standard salbutamol solution was purchased and dissolved into octanol, a standard concentration gradient of salbutamol/octanol solution was configured and the peak values were measured using a UV spectrophotometer, as shown in Fig. S3(a). The solution had absorption peaks at 227 nm and 278 nm and the peaks were proportional to the concentration of salbutamol. Due to the low concentration of salbutamol used in the experiment, the accuracy of the fitted curve at 227 nm was higher, while the fitted curve at 278 nm was chosen in case of high concentration of salbutamol, as shown in Fig. S3(b). Considering the ethical, a medically certified the glass twin-stage impinger lung model was used in the experiment to simulate the human lung absorption, as shown in Fig. S3(c). The impinger stages were filled with ethanol to collect and dissolve the salbutamol–octanol aerosols, and an airflow of 60 L/min was drawn through the impinger during aerosol generation, as shown in Fig. S3(c). At this flow rate, it is estimated that droplets with aerodynamic diameters greater than 5.8 μm are deposited in stage 1, representing the upper respiratory airway walls regions A and B—due to the dominance of inertia in their motion. Droplets with aerodynamic diameters less than 5.8 μm deposit in the lower respiratory airways, i.e., stage 2, which is represented by subregions C1 and C2, due to either diffusion driven molecular collision with lung tissue or gravitational sedimentation.

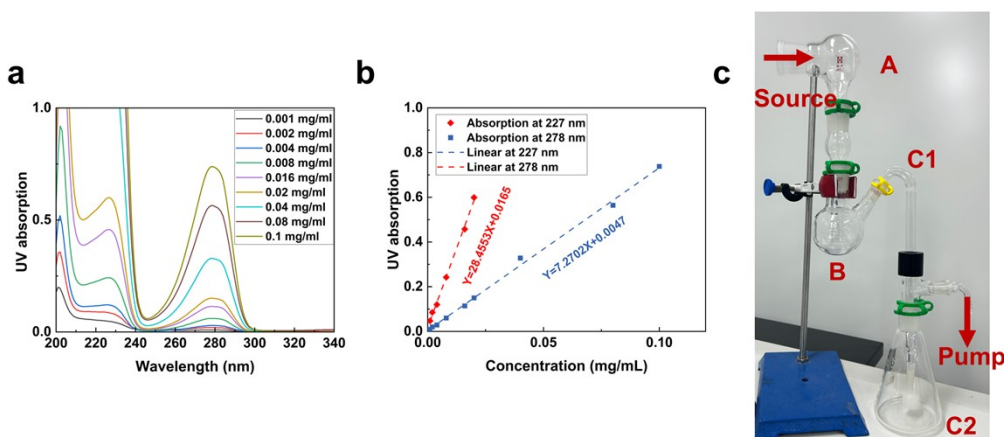


Fig. S3: (a) The UV absorption peaks for solutions with different salbutamol/ethanol concentrations, obtained using UV spectrophotometry. Two absorption peaks are evident, at around 227 and 278 nm.: (b) Calibration curves based on the absorption peaks obtained in (a) used for the dose measurements from the different regions in the lung model. (c) Image of the glass twin-stage impinger lung model employed for the dose measurements. A vacuum pump was connected to the impinger at the marked position to simulate the inhaled air flow. The SAW atomizer is placed at the entrance of the impinger, which constitutes the ‘mouth’ and oral cavity (region A). Region B represents the pharynx and larynx of the upper respiratory tract, and region C, which can be further subdivided into subregions C1 and C2, is a model of the lower respiratory tract including the bronchi and the entire targeted lung area.

4. The non-monotonic response at high power

While further increasing power, exceeding 1.25 W displaced liquid from the resonator's active region, coarsening droplets with two peaks (1.5 W). Although the overall Dv50 is still in the suitable range, the excessively large (>5 μm) particle size results in a reduction of delivery efficiency.

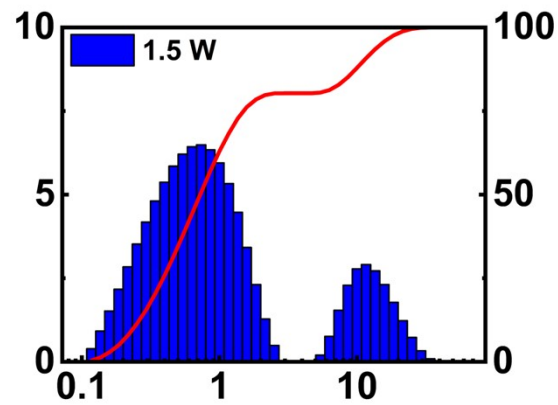


Fig. S4: Droplet size distribution for salbutamol/octanol at 1.5 W. The Dv50 and Dv90 value are 0.7236 μm and 11.17 μm , respectively.

5. Biocompatibility test

Peltier was used to cool the effects of thermal factors. The temperature in the center region of the resonator was 78.5 °C with signal generator at 0.8 W, and 33.6 °C with Peltier, as shown in Fig. S5(a-b). The octanol could still be nebulized well at low temperatures, as shown in Fig. S5(c).

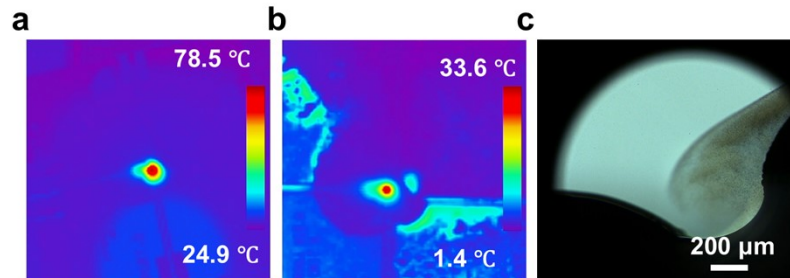


Fig. S5: (a) Image of resonator temperature measured at 0.8 W. (b) Image of resonator temperature measured at 0.8 W with Peltier. The center region was 33.6 °C. (c) Image of nebulization at 0.8 W with Peltier.

6. Heating nebulization

The DC voltage was applied to the GHz acoustic resonator so that only the performance of heating was expressed without the generation of acoustic waves, thus decoupling the heat from the high-frequency acoustic waves and verifying the nature of the nebulization caused. The resistance of the resonator is measured, as shown in Fig. S6(a). In Fig. S6(b), different DC voltages were applied to the resonator and the change in temperature for 30 s of heating was tested using the infrared thermometer. By fitting the graph data, the resonator temperature was positively correlated with the applied voltage, and their relationship was shown in Fig. S6(c). The resonator temperature was measured to be 78.5 °C (Fig. S5) under the excitation of signal generator (0.8 W). Therefore, the 5 V was chosen for heating and observe the nebulization results. As shown in Fig. S6(d), the heating will only make the liquid boil and evaporate, generation large droplets with about 16 μm , which is completely different from the case of GHz acoustic wave nebulization, further verifying the credibility of the mechanism of GHz acoustic waves induced the capillary waves breaking for nebulization.

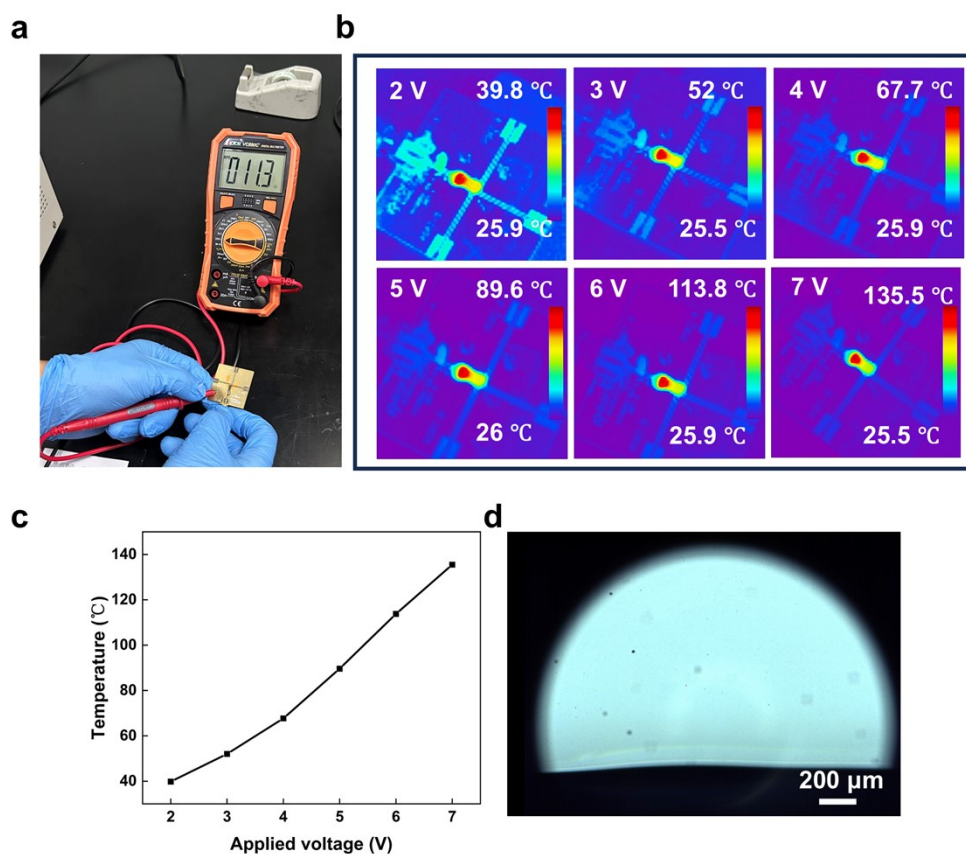


Fig. S6: Heating nebulization. (a) Image of resistance measurement. (b) Images of temperature measurement at different voltages. (c) The relationship between applied voltage and temperature. (d) The photo of evaporating taken by high-speed camera at 5V.

7. Preparation of monodisperse nanoparticles

The preparation of monodisperse nanoparticles has been a challenge due to the aggregation of the particles. Nebulization offers a solution to this, benefitted from the \sim nm droplet sizes. The 500 nm green fluorescent particles were diluted with octanol for nebulization and the results were shown in Fig. S7, the nanoparticles are well received onto the glass substrate.

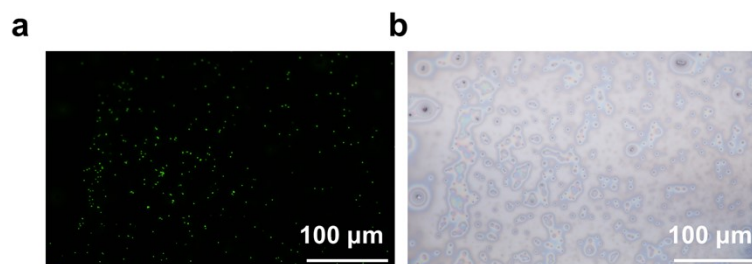


Fig. S7: Preparation of monodisperse nanoparticles: (a) Fluorescent picture of nanoparticles. (b) Bright field images of the nebulized nanoparticles.